Journal of ELECTRICAL ENGINEERING, VOL. 52, NO. 11-12, 2001, 329–337

AN UNCALIBRATED ROBOT SYSTEM FOR REACHING AND GRASPING OBJECTS IN UNPREDICTABLE PHYSICAL ENVIRONMENT

Drago Torkar [*] — **Nikola Pavešić** [**]
Anton Pozne Jr [**] — **Stanislav Kovačič** [**]

This article describes an active stereo vision system which, in combination with a robotic manipulator, is able to perform various visual tasks such as object reaching and grasping. Using the weak perspective camera model, the weakly calibrated stereo vision system, and some heuristics about the robot gripper, the closed-loop visual control of the robot manipulator is generated. Experiments show the robot system based on visual feedback control to be insensitive (robust) to different disturbances of the stereo vision system and robot setup during operation.

K e y w o r d s: active vision, visual robot control, weak perspective, weak calibration, stereo vision

1 INTRODUCTION

A stereo vision system allows robot systems to operate in an unpredictable physical environment. When a robotic manipulator is to be controlled by visual information from a vision system, a transformation between the image space and the manipulator (working) space has to be established.

Conventional approaches to solving this problem are based upon calibrating a vision system with the 3-D environment, determining the object pose, and then grasping the object by the manipulator's gripper, using an open-loop control procedure [16].

The calibration procedure is a time consuming task, which has to be repeated whenever the vision system parameters and/or the robotic manipulator parameters are changed. Moreover, the estimated parameters allow an accurate object pose determination only over a small part of the manipulator working space. Robot systems not requiring calibration are therefore of great practical advantage.

To avoid the precise calibration procedure, techniques were developed to describe a physical environment inaccurately ('weakly'), but sufficiently to perform some visually controlled tasks [4]. In stereo systems, the usual way to obtain weak calibration is to use at least eight point-correspondences between the left and the right image [7, 12] for estimating the elements of the *fundamental matrix* [13, 18], thus defining the epipolar geometry of the system. Using this geometry one can compute relative 3-D point positions [4]. The drawback of this is, again, the need of re-estimating the fundamental matrix , if the system parameters change. This can be circumvented by techniques that can build a weak description of the environment using only available information about the system and information that is quickly obtainable from images.

Visual information from images can provide closed-loop position control for a robot end-effector, also known as visual servoing [3]. Algorithms presented in the literature differ regarding the definition of the error signal and/or the way the visual information is used to control the robot. If the error signal is defined in 3D robot coordinates, the approach is referred to as *position based*. Although it is insensitive to calibration errors and minor changes of camera positions, a camera and a target model are needed and a sort of quick self calibration or on-line calibration procedure is necessary [8]. If the control values are computed on the basis of image features directly, the servoing is denoted as *image-based*. Sometimes, the error signal is computed from optical flow [5]. In the *look-and-move* systems, the vision provides the inputs to the joint level controller of the robot manipulator. Since robot controllers already solve many kinematic and dynamic problems, most of the visually controlled systems are of this type [17, 6]. In contrast, if the visual controller replaces the robot controller entirely and directly controls the robot joints, the system is known as *direct visual servo*; this is rarely used [11].

A new approach to the realization of a robot system not requiring calibration is presented here. It is based upon an inaccurate ('weak') simultaneous determination of the object and manipulator's gripper poses, and on the use of a closed-loop control algorithm to reach the object with the manipulator's gripper. The error signal is interpreted in robot coordinates (position-based approach), and control values are passed on to the robot controller

[*] Jožef Stefan Institute, Jamova 39, Ljubljana, e-mail: drago.torkar@ijs.si
[**] Faculty of Electrical Engineering, Tržaška 25, Ljubljana, e-mail: {tonep, stanek, nikolap}@fe.uni-lj.si

ISSN 1335-3632

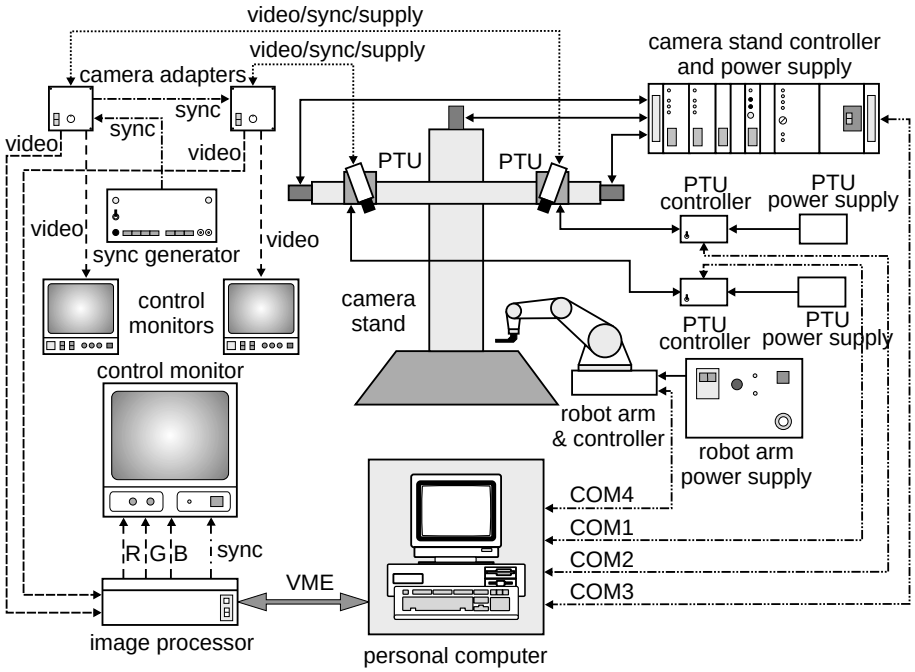

Fig. 1. Experimental active vision system setup

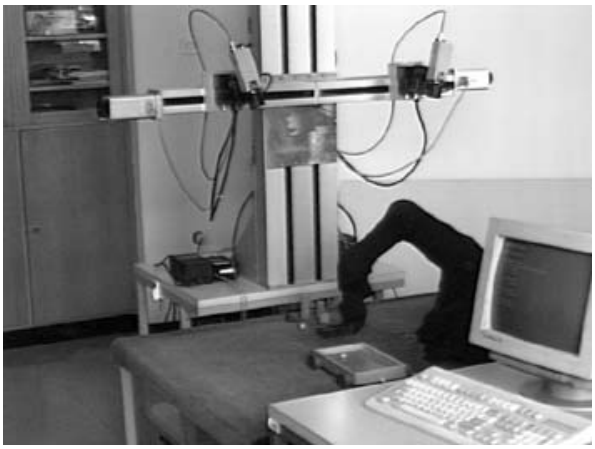

Fig. 2. Photography of the laboratory active stereo vision system

(look-and-move system). The main advantage over similar systems lies in the fact that no calibration procedure of any kind takes place. The available information about the system and some image features are used instead.

This paper is organized as follows: In Section 2 a brief system overview and a short description of its most important parts are given. Section 3 introduces the idea of weak perspective and its implementation in the stereo vision system. In Section 4, a description of each step in the process of visually guided object grasping is given. In Section 5, we present the system behaviour and some results obtained so far. Section 6 concludes the paper.

2 EXPERIMENTAL SETUP

Our experimental system consists of an active stereo camera system, a robotic manipulator, an image processor and a personal computer (Fig. 1). The active stereo camera system is based on a motorized camera stand, built from ISEL linear drives, and two pan-tilt units (PTU), manufactured by Directed Perception. The camera stand enables adjustment of the vertical position of the camera pair from 0 mm to 800 mm, resulting in the distance between the cameras and the robot's workspace to be between 400 mm to 1200 mm. The horizontal positioning range for each camera is 315 mm. This allows the baseline distance to be set between 200 mm and 830 mm. Positioning accuracy for each linear drive is better than 0.01 mm.

To control the gaze direction of the two cameras, the camera stand is equipped with two camera pan-tilt units. The pan angle range is 318° and the tilt angle range 78°. Maximum rotation speed for both axes is over 300° per second. The controllers of the pan-tilt unit allow different operating modes to be set, such as coordinated movement of pan and tilt axes, adjustment of acceleration profiles, *etc.* All motors in the camera stand drives and the pan-tilt units are steppers. Since the camera stand and the pan-tilt units have no built-in absolute position sensors, the system must be initialized (set to home position) before use.

Two B/W CCD cameras (SONY type AVC-D7CE) are attached directly to the pan-tilt units. Each camera is equipped with an automatic iris/manual focus lens. Camera outputs are connected to separate video inputs of the

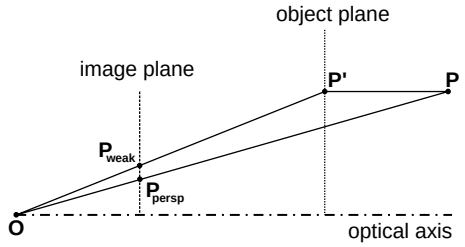

Fig. 3. The weak and full perspective projections of an arbitrary object point.

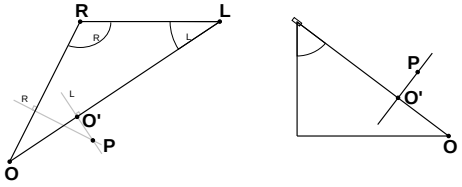

Fig. 4. Geometry of the stereo weak perspective

Imaging Technology 151 image processor. Both cameras are externally synchronized in order to minimize input video multiplexer switching time. The image processor is used to grab and binarize the camera images and to perform some low-level image processing tasks. The robotic manipulator Rob3i, manufactured by P&P Elektronik, has five degrees of freedom and a motorized gripper. The joints are driven by DC servo motors. The positioning resolution is rather low — about 3.5 mm in the worst case (manipulator fully stretched). The original form of the gripper jaws was not suitable for visual robot control. Newly designed and enlarged black painted gripper jaws [15] with white stripes on the top edge enable the robot vision system to see the gripper during the object reaching phase. The manipulator and the surface of the table are covered with dark textile (Fig. 2) to avoid reflections and to simplify segmentation of the camera images. During the experiments, additional light sources were used to illuminate the robot's workspace.

An IBM-compatible PC is used to control the gaze direction of the cameras and the position of the manipulator. Controllers of the camera stand, pan-tilt units and the robot arm are connected to a host PC via RS232 ports (Fig. 1).

3 WEAK PERSPECTIVE CAMERA MODEL

Assuming the classical full-perspective camera model, the relations describing the mapping of a robot space point (an object point) to the image plane are *nonlinear*. A weak perspective camera model represents a zero order approximation of the full perspective camera model [10]; geometrically, it assumes that the object points lie on a plane (usually called *object* plane) parallel to the image plane. Since all points on an object plane lie at the same distance from camera's perspective center, the mapping between world and image coordinates becomes *affine* and can be modeled by scaling.

In Figure 3, it can be seen that by using the weak perspective instead of the full perspective projection of an object point cause an erroneous projection of the point, which is geometrically equal to the distance $\mathbf{P}_{weak}\mathbf{P}_{persp}$. While this error decreases as the object point $\mathbf{P}$ gets closer to the plane approximating the object (object plane) or to the optical axis, the weak perspective camera model will be an appropriate approximation of the full perspective model providing that the object lies in the neighbourhood of the camera optical axis.

Using the weak perspective camera model has some advantages over using the full perspective one [2]. The weak perspective model is conceptually simpler since it uses orthographic instead of perspective projection and it doesn't require the knowledge of camera intrinsic parameters. It is a linear model therefore, the computations involved are less complicated than with a non-linear full perspective model. The scale factor is incorporated in the weak perspective model itself, and it can be used without modification to recognize a scaled version of an object.

4 WEAK PERSPECTIVE MODEL OF AN ACTIVE STEREO VISION SYSTEM

Adopting the weak perspective camera model to model the cameras of our stereo system, the cameras are controlled in such a way that their optical axes intersect in or pass close to the point of interest (Fig. 4). The optical centers of the two cameras ($\mathbf{L}$, $\mathbf{R}$) and the first point of interest $\mathbf{O}$ (object's center of gravity) form a triangle of constantly changing area and angles, as the point $\mathbf{O}$ moves across the robot workspace. The angles Θ_L and Θ_R are calculated from the pan (φ) and tilt (ϑ) angle of the two cameras [15]:

$$\cos\Theta = \cos\vartheta \sin\varphi\,. \tag{1}$$

Observing Figure 3, one can notice that the weak perspective error on the image plane would be zero if the point $\mathbf{P}$ lay on the object plane ($\mathbf{P} = \mathbf{P}'$) or on the optical axis; thus the overall error would be minimized. Therefore, we define the two object planes Π (left and right) as both passing through the second point of interest $\mathbf{P}$ (gripper's center of gravity). The left camera optical axis perpendicularly intersects the plane Π_L and the right camera optical axis perpendicularly intersects the plane Π_R. The triangle $\mathbf{LRO}$ lies on the plane Σ perpendicular to both object planes Π. The inclination angle δ in Fig. 4 is calculated from pan and tilt angles, regardless of the camera [15]:

$$\tan\delta = \frac{\tan\vartheta}{\cos\varphi}\,. \tag{2}$$

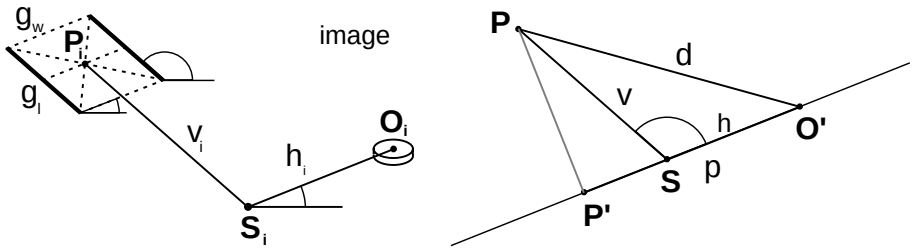

Fig. 5. Image representation of the gripper and object

5 CLOSED–LOOP CONTROL APPROACH

In order to move the manipulator's gripper close to the object which should be grasped, both the robot gripper and the object must be accurately detected in the left and right image. Following the scheme described in Section 4, the vergence control is necessary to keep the optical axes of the cameras near to the object. After analyzing the abilities of the available system, especially the abilities of the robotic manipulator and the image processor, a look-and-move approach of visual control [3] was implemented, therefore all actions are performed sequentially.

5.1 Camera Vergence Control

The goal of the camera vergence control system is to generate camera movements that compensate for vergence errors. This is achieved by two independent control loops for each camera, controlling the pan and tilt movements [14]. The vergence control loop consists of three stages: image digitalization, error estimation and error correction. Error is defined in the sense of image distance of the object's center of gravity to the center of the image. Since the camera stand is aligned with the robot coordinate system in a way that the baseline **LR** is nearly parallel to the y axis of the robot coordinate frame, tilt movement is used to correct the vertical image position and pan movement is used to correct the horizontal one. The vergence system is active all the time during the system operation to compensate for the movements of the object or the camera stand during task performance.

5.2 Mapping from Image to Object Plane

To locate the manipulator gripper and the candidate object for grasping, the size, orientation, and gravity centers of all objects in both images are determined. Parallel gripper jaws are marked with rectangular white stripes on the top edge. They appear in the image as oblong objects and are checked pairwise for parallelism determine the gripper candidates. If two corresponding objects are found, the average of their centers of gravity defines the gripper position.

The candidate object for grasping is selected as the smallest of all objects on the scene, having an area above the threshold.

The length of the white stripes on the gripper jaws is approximately the same as their opening. The stripes form a virtual square with two sides parallel to the x-axis of the robot coordinate frame and two sides parallel to y-axis. Under oblique camera viewing angles this square is seen by the cameras as a parallelogram using the weak perspective model [15]. Two parallel sides of length g_l reflect the x world axis direction in the image and the other two of length g_w the y direction. The separation between gripper center $\mathbf{P}_i$ and object center $\mathbf{O}_i$ is decomposed into two segments, one with orientation α and the other with orientation β (Fig. 5).

5.2.1 Scaling Factor

According to the weak perspective camera model the points and lines seen in the camera image are a scaled version of all the points and lines on the virtual plane Π passing through the gripper's center of gravity. There are two directions in the image reflecting the world's x- and y-axes; therefore not one, but two different scale factors (λ_l, λ_w) have to be determined. In our case, they are determined from the known length G_l of the white stripes on the top of the robot gripper jaw and the jaw opening distance G_w. Those stripes lie in a plane parallel to xy plane of the robot coordinate system and are aligned with the x-axis. In the image processing stage, the length of the stripes g_l and the jaw opening g_w are measured in the image.

The ratios $\frac{G_l}{g_l}$ and $\frac{G_w}{g_w}$ can not be used directly because the inclination of g_l and g_w towards x- and y-axes has to be considered. The scaling factors are

$$\lambda_l = \frac{G_l}{g_l}\cos\vartheta\,, \qquad \lambda_w = \frac{G_w}{g_w}\sin\Theta\,. \tag{3}$$

The mapping from the image onto the Π plane in general does not preserve the orientation angles α and β. This is due to sampling errors which we neglected. With the help of the angle γ the projection p of the line

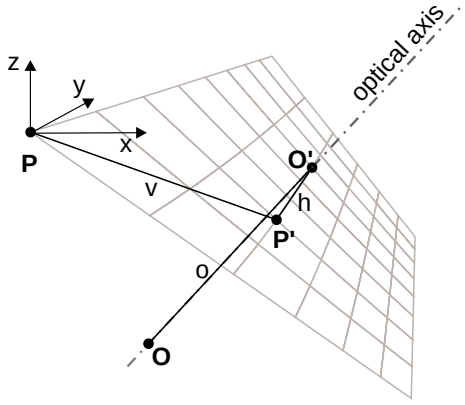

Fig. 6. Path segments between the gripper and the object

segment d to the intersection between planes Σ and Π is calculated.

5.3 Mapping from Object Plane to Robot Workspace

The path that the manipulator's gripper has to travel to grasp an object, is depicted in Fig. 6. Point **P** lies on the virtual object plane Π described in Section 3. The gripper must travel from this point to the point **O**. The first two segments of the path (v and h) lie on the object plane. The third segment (o) lies along the optical axis and is computed from the information extracted from both stereo images. Since the camera-centered coordinate frame is rotated and translated in relation to the robot frame, all three segments contribute to the x, y and z direction of the robot movement.

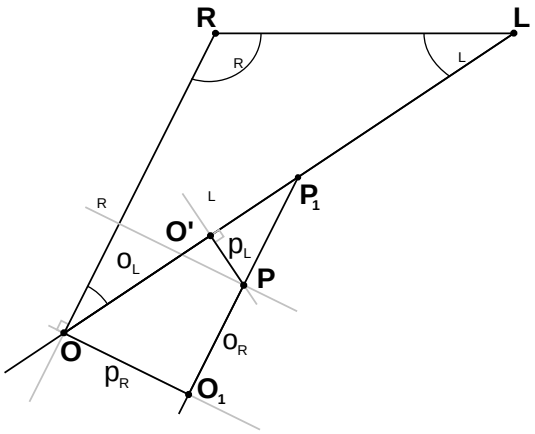

Fig. 7. Calculating the distance between object **O** and plane Π_L

5.3.1 Segment Decomposition

The three path segments of the object-to-gripper separation must be decomposed into the x, y and z direction of the robot coordinate frame in order to obtain an estimation for each direction controller. Segments v and h lie on the plane Π. Their lengths are recovered from images using scale factors (Equation 3). The length of the segment o must be calculated using information from both object planes Π (Fig. 7).

$$o = \frac{p_R - p_L \cos\nu}{\sin\nu}\,, \qquad \nu = \pi - \Theta_L - \Theta_R\,. \tag{4}$$

The lengths of the three segments are now known, and by considering the inclination angles of the robot coordinate axes towards planes Π and Σ and the orientation of the optical axes and segments themselves, projections of the segments to the robot coordinate axes can be computed. Some of the angles involved in the computation, like Θ and δ, are obtained from the camera orientation angles, *ie*, pan and tilt, and the others, like γ, are obtained from the images. Only one object plane Π (left or right) can be used to get segments v and h and corresponding x, y and z projections. From the other object plane, only the segment d is used to calculate segment o on the optical axis. Calculations for both Π planes and object axes can be used to smooth the errors. The sign of a particular segment depends on the mutual positions of points **P** and **O**. The path segment o yields the following contributions:

$$\begin{gathered}\Delta x_o = o\ \sin\Theta\sin\delta\,, \quad \Delta y_o = o\ \cos\Theta\,,\\ \Delta z_o = o\ \sin\Theta\cos\delta\,,\end{gathered} \tag{5}$$

the segment h yields

$$\begin{gathered}\Delta x_h = h\cos\Theta\sin\delta\,, \quad \Delta y_h = h\sin\Theta\,,\\ \Delta z_h = h\cos\Theta\cos\delta\,,\end{gathered} \tag{6}$$

and the segment v produces:

$$\begin{gathered}\Delta x_v = v\ \cos\vartheta\,, \quad \Delta y_v = v\ \cos\gamma\sin\Theta\,,\\ \Delta z_v = v\ \sin\vartheta\cos\varphi\,.\end{gathered} \tag{7}$$

Estimates for the x, y and z movements are summed and passed to the three controllers, one for each axis. Since positioning the gripper point **P** onto the object point **O** is not possible (due to occlusions caused by the gripper jaws approaching the object and possible hitting of the object by the gripper) the reference point for the x controller is intentionally offset by the distance D_x from the object point **O** in the direction of the coordinate origin. Finally, control rules for each axis are generated:

$$\begin{aligned}\Delta x &= K_x(\Delta x_o + \Delta x_h + \Delta x_v - D_x)\,,\\ \Delta y &= K_y(\Delta y_o + \Delta y_h + \Delta y_v)\,,\\ \Delta z &= K_z(\Delta z_o + \Delta z_h + \Delta z_v)\,.\end{aligned} \tag{8}$$

Table 1. Results of the grasping experiment

	$\delta = 0^o - 5^o$			$\delta = 13^o - 17^o$			$\delta = 23^o - 27^o$		
n	succ.	$\overline{err.}$ (mm)	$\overline{rep.}$	succ.	$\overline{err.}$ (mm)	$\overline{rep.}$	succ.	$\overline{err.}$ (mm)	$\overline{rep.}$
20	95 %	1.8	7.5	60 %	1.9	6.2	70 %	2.3	7.7

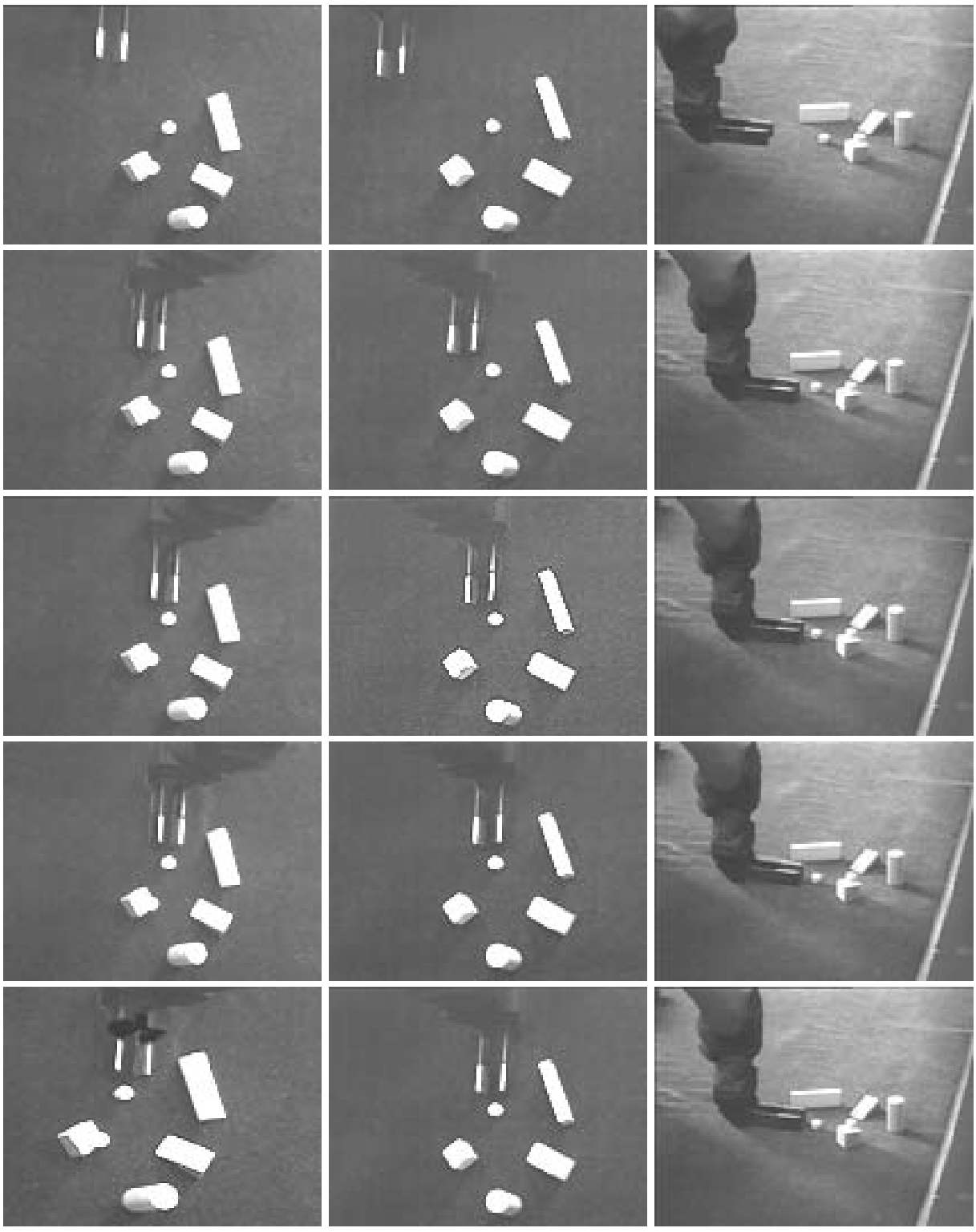

Fig. 8. Gripper approaches the reference point.

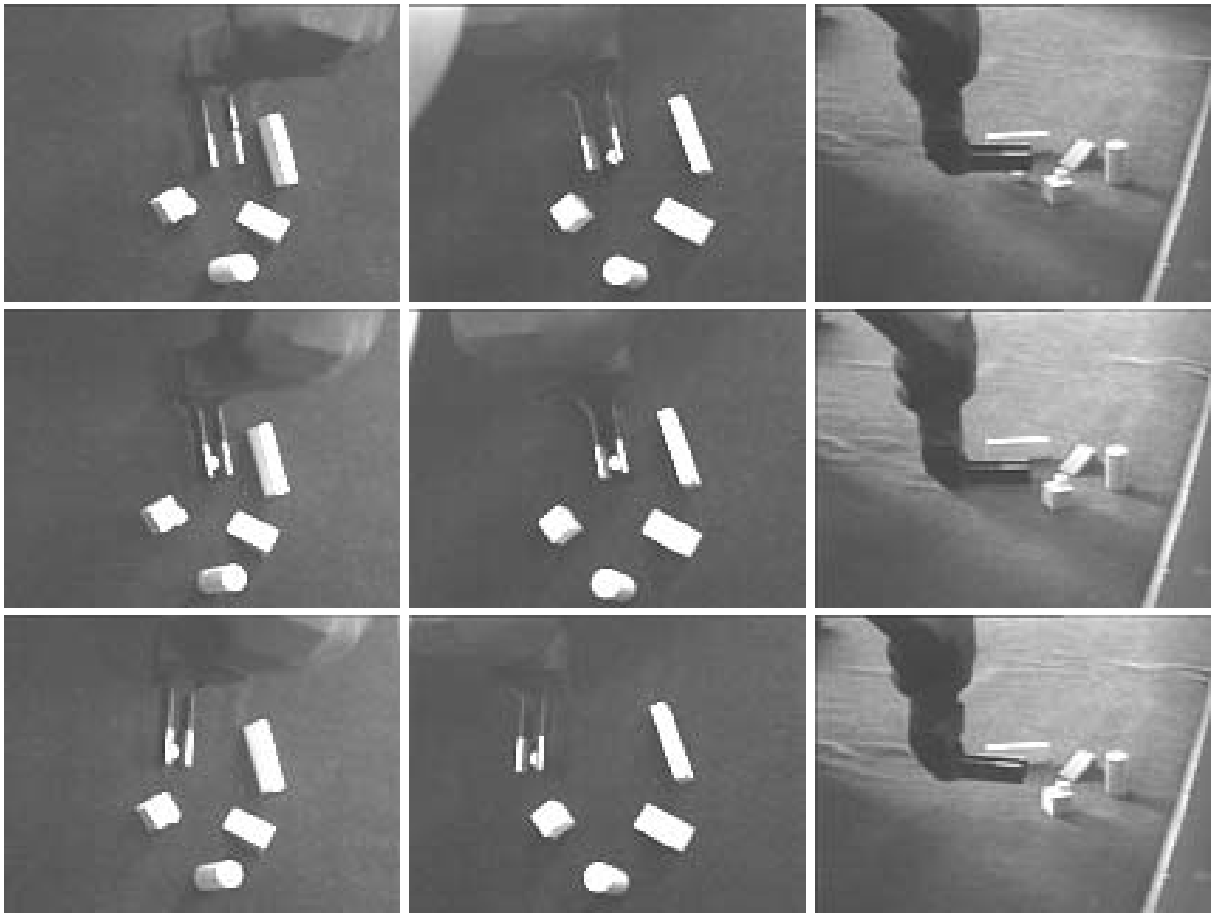

Fig. 9. Ballistic grasp.

Proportional gain coefficients K_x, K_y and K_z, set to values less than 1, compensate for the errors and prevent instability in the manipulator movement. When the robot gripper successfully reaches the reference point, the following take place: firstly, the size of the object in the direction of gripper opening is determined; secondly, the visual control is turned off and the gripper moves above the object; finally, the gripper moves vertically downwards until the appropriate height is reached, the opening of the jaws is adjusted, and the jaws grasp the object.

6 SYSTEM IN ACTION

The initial system setup demands an object to be visible by both cameras and to be in or moving towards the robot workspace. The locations of the cameras are arbitrary except that they must both observe the common area where the object is to appear. The cameras lock on the object and track it until it stops. The robot gripper is then moved into the workspace, and both the object and the gripper must be seen by the cameras. If not, the gripper systematically moves around inside its workspace until it comes into the viewing area. In that moment, the grasping action starts. The grasp control loop starts by grabbing and proceeds by binarization and segmentation of the image stereo pair. Points $\mathbf{O}_i$ and $\mathbf{P}_i$ are located and initial gripper-to-target separation in robot coordinates is computed and passed to the x, y, and z controllers.

The controllers first calculate directional movements and second, if these movements are small enough, enable ballistic grasp action. If the movements are not small enough, the controllers move the manipulator to the new position. If the grasp action was not enabled, the control is passed to the outer verging loop that checks the object position. If it is different from the last known position, camera orientations are adjusted. Figure 8 shows an example of the manipulator movements during an approach to the reference point. When reached, as shown in Fig. 9, the system can grasp the object in an open-loop manner, without looking. This is achieved in two steps: first the gripper moves above the object to prevent it from being accidentally hit and moved, and then it descends to an appropriate height with the jaws fully apart. The dimension of the object is estimated with the help of λ_β and the opening of the jaws is adjusted accordingly.

The grasp control loop runs at 2.5 to 3 Hz. Typically 6 to 8 repetitions are needed before the reference point is reached. Occasionally, low positioning resolution of the manipulator causes problems and the gripper oscillates around the reference point. In Fig. 10, two cases of the approach are depicted. On the left graph a typical sit-

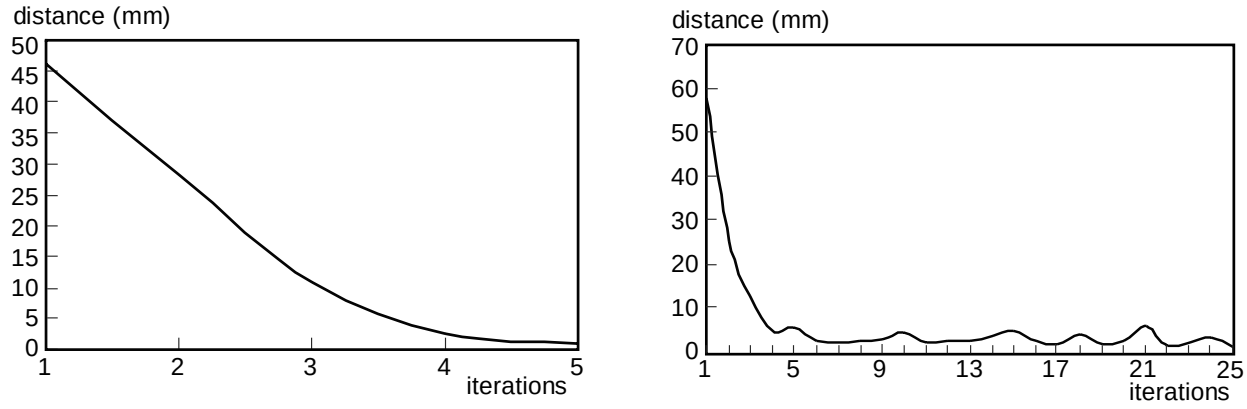

Fig. 10. Smoothed approach of the gripper to the reference point

uation is shown where the control loop stopped after 5 iterations. The right graph represents an extreme situation where the gripper oscillated around the reference point and the loop ended after 25 repetitions.

To test the ability of the system and the described control algorithm a cylindrical object ($h = 10$ mm, $d = 15$ mm) was placed in the robot's workspace sixty times at different heights and different distances to the gripper. The camera stand was moved to three different distances from the edge of the robot's basic workplane resulting in three different ranges of the angle δ (see Fig. 4). The maximum gripper opening (32 mm) enabled the object to be picked up easily. This is why some inaccuracy of gripper positioning to the reference point was allowed (1 mm in each direction). Besides the number of successfully accomplished grasps and the number of loop repetitions, the absolute distance between the gripper position and the reference point, which was placed 40 mm in x direction before the object, was measured. This error is caused by image segmentation, the weak perspective model, and weak calibration. The average values of this error and the average number of loop repetitions for each range of angle δ are presented in Tab. 1.

7 CONCLUSION

In this paper an active stereo vision system and a closed loop visual control algorithm, which is able to perform object grasping and manipulation by knowing only a few facts about the system, are presented. Instead of system calibration or self calibration, only available information and some constraints were used to visually guide the manipulator gripper to the target. Pan and tilt angle orientations of stereo cameras, the length of the fiducial marks on the gripper jaws, and the gripper opening are the only absolute values available to the control algorithm. By placing the object plane Π through the gripper's center of gravity and by verging the optical axes of stereo cameras in a way to intersect in, or pass through, the nearest neighborhood of an object's center of gravity, the systematic error of the weak perspective model was minimized. Errors, which are successfully overcome by visual feedback gain, do not significantly reduce the system performance.

References

[1] ALOIMONOS, Y.—WEISS, I.—BANDYOPADHYAY, A.: Active Vision, In Proc. 1st Int. Conf. on Computer Vision, 35–54, 1987.

[2] ALTER, T. D.: 3D Pose from 3 Corresponding Points under Weak Perspective Projection, A.I. Memo No. 1378, MIT, July 1992.

[3] HUTCHINSON, S.—HAGER, G.—CORKE, P. I.: A Tutorial on Visual Servo Control, Technical Report RR-1068, Yale University, 1995.

[4] ROBERT, L.—FAUGERAS, O.: Relative 3D Positioning and 3D Convex Hull Computation from a Weakly Calibrated Stereo Pair, Image and Vision Computing **13** No. 3 (1995), 189–196.

[5] GROSSO, E.—METTA, G.—ODDERA, A.—SANDINI, G.: Uncalibrated Visual Servoing in Reaching Tasks, Technical Report TR 3-95, LIRA, University of Genova, 1995.

[6] HAGER, G. D.—CHANG, W. C.—MORSE, A. S.: Robot Hand-Eye Coordination Based on Stereo Vision, IEEE Control Systems (1995), 30–39.

[7] HARTLEY, R. I.: In Defence of the Eight-Point Algorithm, IEEE Tran. on Pattern An. and Mach. Intell. **19** No. 6, 580-593.

[8] HOLLINGHURST, N.—CIPOLLA, R.: Uncalibrated Stereo Hand-Eye Coordination, Image and Vision Computing **12** No. 3 (1994), 187–192.

[9] HOLLINGHURST, N.: Uncalibrated Stereo Vision and Hand-Eye Coordination, PhD thesis, University of Cambridge, Department of Engineering, 1997.

[10] HORAUD, R.—CHRISTY, S.—DORNAIKA, F.: Object Pose: the Link Between Weak Perspective, Para Perspective, and Full Perspective,, Technical Report No. 2356, INRIA, September 1994.

[11] JÄGERSAND, M.— NELSON, R.: Adaptive Differential Visual Feedback for Uncalibrated Hand-Eye Coordination and Motor Control, Technical report TR-579, University of Rochester, Department of computer science, 1994.

[12] LONGUET-HIGGINS, H. C.: A Computer Algorithm for Reconstructing a Scene from Two Projections, Nature **293** (1981), 133–135.

[13] LUONG, Q.-T.—DERICHE, R.—FAUGERAS, O.—PAPADOPOULO, T.: On Determining the Fundamental Matrix: Analysis of Different Methods and Experimental Results, Technical Report RR-1894, INRIA, 1993.

[14] POZNE, A.: Sledenje objekta z vizualno povratno zanko, In Proc. ERK'95 vol. B (In Slovene), Portorož, pp. 277-280, 1995.

[15] POZNE, A.: Doseganje predmetov v prostoru z neumerjenim sistemom aktivnega vida, Master's thesis (in Slovene), Univerza v Ljubljani, Fakulteta za elektrotehniko, 1997.

[16] YOSHIMI, B. H.—ALLEN, P.: Alignment Using Uncalibrated Camera System, IEEE Tran. on Robotic and Automation **11** No. 4 (1995), 516–521.

[17] YOSHIMI, B. H.—ALLEN, P.: Closed-Loop Visual Grasping and Manipulation, Proc. of IEEE International Conference on Robotics and Automation, 1996.

[18] ZHANG, Z.—DERICHE, R.—FAUGERAS, O.—LUONG, Q.-T.: A Robust Technique for Matching Two Uncalibrated Images through the Recovery of the Unknown Epipolar Geometry, Technical Report RR-2273, INRIA, 1994.

Received 16 March 2001

Drago Torkar (PhD), was born in 1964. He received the BS degree, the MS degree and the PhD degree in Electrical Engineering from the Faculty of Electrical Engineering, University of Ljubljana, Slovenia in 1990, 1995 and 1998, respectively. He has been with the Department of Computer Systems, Jozef Stefan Institute, since 1991. His research interests include active computer vision, machine vision and pattern recognition.

Nikola Pavešić (Prof, PhD), was born in 1946. He received the BS degree in Electronics, the MS degree in Automatics and PhD degree in Electrical Engineering in 1970, 1973 and 1976, respectively. Since 1970 he has been a staff member at the Faculty of Electrical Engineering, University of Ljubljana, Slovenia, where he is currently a Full Professor for Systems, Automatics and Cybernetics, Head of the Laboratory of Artificial Perception. His research interests include pattern recognition and image processing, speech recognition and understanding and theory of information. He has authored and co-authored more than 100 papers and 3 books addressing several aspects of the above areas.

Anton Pozne Jr (MSc), was born in 1969. He received the BS degree and the MS degree in Electrical Engineering from the Faculty of Electrical Engineering, University of Ljubljana, Slovenia in 1994 and 1997, respectively. He is currently studying toward the PhD degree. His principal research interest is active robot vision.

Stanislav Kovačič (Prof, PhD), was born in 1952. He received the BS degree, the MS degree and the PhD degree in Electrical Engineering from the Faculty of Electrical Engineering, University of Ljubljana, Slovenia in 1976, 1979 and 1990, respectively. There he is currently an Associate Professor and Head of Machine Vision Group. His research interests are active vision, robot vision, industrial imaging, visual inspection, biomedical imaging, segmentation and multi-scale approaches.